İstanbul Üniv. Vet. Fak. Derg.
39 (1), 67-75, 2013
Araştırma Makalesi

J. Fac. Vet. Med. Istanbul Univ.
39 (1), 67-75, 2013
Research Article

Radiological and Ultrasound Imaging Scores in Experimental Sodium Monoiodoacetate Model of Knee Osteoarthritis in Dogs

Nikolay GORANOV[1], Mihail PASKALEV[1], Dian KANAKOV[2]*

[1]Department of Veterinary Surgery, Faculty of Veterinary Medicine, Trakia University, 6000 Stara Zagora, Bulgaria
[2]Department of Internal Diseases, Faculty of Veterinary Medicine, Trakia University, 6000 Stara Zagora, Bulgaria

**Corresponding Author: N. V. GORANOV, Department of Veterinary Surgery, Faculty of Veterinary Medicine, Trakia University, 6000 Stara Zagora, Bulgaria*
e-mail: nickgoranov@yahoo.com

Geliş Tarihi / Received: 27.10.2011

ABSTRACT

Experimental osteoarthritis was induced in six adult dogs by intraarticular injection of sodium monoiodoacetate in left knee joints. The contralateral knees served as control. The changes occurring in joints were followed out by radiography and ultrasound imaging in the beginning (day 0), and on post injection days 30, 60, and 105. Two assessment systems were used to generate individual scores for each time interval. The results evidenced dynamic and consistently increased scores for left joints in both diagnostic imaging techniques used with statistically significant differences between left and right joints. Radiological and ultrasound scores were closely correlated ($r=0.55$, $P<0.001$) suggesting that the combined use of both imaging techniques was more advantageous for diagnostics of osteoarthritis.

Key Words: Dogs, knee joint, sodium monoiodoacetate model, radiography, ultrasonography, osteoarthritis

ÖZET

KÖPEKLERDE DİZ OSTEOARTRİTİNİN DENEYSEL SODYUM MONOİYODOASETAT MODELİ İLE RADYOLOJİK VE ULTRASONOGRAFİK GÖRÜNTÜLEME SKORLARI

Çalışmada, sodyum monoiyodoasetatın altı adet yetişkin köpeğin sol diz eklemine intraartiküler enjeksiyonu ile deneysel osteoartrit oluşturuldu. Kontralateral dizler kontrol olarak ayrıldı. Başlangıçta (gün 0) ve enjeksiyonu takip eden 30., 60. ve 105. günlerde radyografi ve ultrasonografik görüntülemelerle eklemlerde meydana gelen değişiklikler incelendi. Bireysel skorlar elde edilmesinde her bir zaman aralığı için iki değerlendirme sistemi kullanıldı. Kullanılan her iki diagnostik görüntüleme tekniklerinde istatistiksel olarak sağ ve sol eklemlerde önemli farklılıkların olduğu ve sonuçlar sol eklemlerdeki skorun istikrarlı bir şekilde artış gösterdiği ortaya çıkardı. Radyolojik ve ultrasonografik skorlarının korelasyon ($r=0,55$; $P<0,001$) sonuçlarına göre görüntüleme tekniklerinin birlikte kullanılmasının osteoartrit tanısı için daha avantajlı olduğunu saptanmıştır.

Anahtar Kelimeler: Köpek, diz eklemi, sodyum monoiyodoasetat modeli, radyografi, ultrasonografi, osteoartirit

Introduction

Osteoarthritis (OA) is a degenerative disease of articular cartilage encountered in all mammalian and avian species, and men (Lipowitz, 1993). Ehrlich (2003) and Haima (2005) define it as a dynamic cartilage "wear-and-tear" process. Martel-Pelletier (1999) described sclerosis of subchondral bone and involvement of synovial membrane. The etiology of OA is multifactorial (Grainger and Cicuttini, 2004) and the general outcome is a various degree of cartilage loss, bone remodelling, pain, effusion and loss of activity. OA is rather a syndrome, than a separate diseases (Buckwalter and Martin, 2006) characterized with slow progress, worsening of cartilage quality, formation of osteophytes, subchondral bone remodelling, periarticular tissue changes, low-extent inflammation.

Conventional radiography is an excellent method for examination of bones, but yields few information for what is going on in soft tissues (Carring, 1997; May, 1994). A "blind spot" is the inability for direct visualization of the cartilage (Railhac and Vial, 2007). Yet, the method was assessed as more informative for bone tissue than magnetic resonance imaging and computed tomography (Van Bree, 2006). The typical radiological findings in OA are osteophytes, bone sclerosis, cysts and subluxations (Abercromby et al., 2006; Boulos et al., 2003; Swagerty and Hellinger, 2001). The complete destruction with ankylosis is rare. The articular cartilage and menisci are not visible, but indirectly assessed by the intraarticular space. Early changes however, are not recorded on radiographs. The interpretation of findings in animals is even more difficult, subjective and more reliable by calculating a total score from each observed sign (Lazar et al., 2005). More information could be obtained by special radiological techniques, excellent technical performance and especially, comparison with the contralateral limb (Bennett et al., 1988; Carring, 1997; Robins, 1990; Torelli et al., 2005; Vasseur, 1993).

The ultrasonography (USG) of knee joint is a non-invasive, not expensive and readily available diagnostic imaging technique (Comeford, 2006; Kramer et al., 1999), yet with limited application in small animals (Budsberg and Thomas, 2006). Nevertheless, USG is faster, painless and safer than radiography or arthroscopy, and requires neither strict aseptics nor general anaesthesia (Kil-Ho Cho et al., 2001).

B-mode USG with 5-10 MHz transducers are recommended for examination of canine knee joint to visualize structure up to 4 cm in depth (Kramer et al., 1997; Muller and Kramer, 2003; Reed et al., 1995). The most commonly used acoustic window is the sagittal one - laterally to the patellar ligament. Disadvantages of the method are the insufficient resolution with regard to small cartilage defects and the acoustic shadowing from the subchondral bone. The 20 MHz transducers achieve a remarkable axial resolution of 0.038 mm but the maximum possible depth is 1.5 cm (Grassi and Cervini, 1998).

Kramer et al. (1999) are convinced that comparable USG findings in canine knee joint are possible only if a standard algorithm is used. Reed et al. (1995) described the normal echographic anatomy of the joint in dogs. The cartilage, affected by OA, shows a wide range of findings, from extensive to very subtle structural changes (Grassi and Cervini, 1998). The loss of the sharply delineated boundary between cartilage and soft tissues is indicative when other signs are absent. The visualization of fluid collection and increased echogenicity (hypertrophy) of synovial membrane are an advantage of USG compared to radiography (Grassi and Cervini, 1998).

The radiography and ultrasound imaging findings in experimental osteoarthritis of the knee, induced by sodium monoiodoacetate in dogs are not reported. The aim of the present study was to monitor the time course of occurring changes and to investigate the potential of combined application of both imaging techniques for diagnostics of OA in dogs.

Materials and Methods

Experimental animals

Six clinically healthy mongrel dogs from both sexes were used (body weight 15±2 kg). They were housed in individual boxes indoor with free access to drinking water and dry canine food for maintenance. The experiment was approved by the Committee on Animal Experimentation at the Trakia University, Stara Zagora, Bulgaria and was performed in strict compliance with animal welfare regulations (Directive 86/609/EEC).

Osteoarthritis experimental model

Over ten weeks, intraarticular injections of sodium monoiodoacetate (MIA) (Merck, Germany) were performed once weekly in left stifle joints at doses of 0.12, 0.14, 0.16, 0.26, 0.36, 0.96, 1.28, 3.00, 5.00 and 10.00 mg/kg in 1 ml 0.9% saline solution. The right joint served as control.

Table 1. Parameters for calculation of radiographic osteoarthritis score (Lazar et al., 2005).
Tablo 1. Radyografik osteoartrit skor hesaplama parametreleri (Lazar ve ark., 2005).

Stifle component	Radiographic features
Patella	1) Apical osteophytes (ML)
	2) Basal osteophytes (ML)
	3) Cranial apical enthesophytes (ML)
Femur	4) Trochlear groove periarticular osteophytes (ML)
	5) Supratrochlear lesions (ML)
	6) Fabellar periarticular osteophytes (ML)
	7) Subchondral sclerosis (AP)
	8) Remodelling of the distal femoral condyle (AP)
	9) Subchondral cysts of femoral metaphysis (AP)
	10) Subchondral cysts of indercondylar fossa (AP)
	11) Subchondral cysts of the condyle (AP)
	12) Lateral condylar periarticular osteophytes (AP)
	13) Medial condylar periarticular osteophytes (AP)
	14) Osteophytes at the lateral collateral ligament (AP)
	15) Osteophytes at the medial collateral ligament (AP)
Tibia	16) Cranial periarticular osteophytes (ML)
	17) Caudal periarticular osteophytes (ML)
	18) Subchondral cysts (ML)
	19) Remodelling of the condyle (ML)
	20) Osteophytes of the central tibial plateau (ML)
	21) Medial periarticular osteophytes (AP)
	22) Lateral periarticular osteophytes (AP)
	23) Medial subchondral sclerosis (AP)
	24) Lateral subchondral sclerosis (AP)
	25) Intercondylar osteophytes (AP)
Soft tissues	26) Joint effusion or thickening (ML)
	27) Lateral soft tissue thickening (AP)
	28) Medial soft tissue thickening (AP)
Other aspects of the stifle joint	29) Intracapsular mineralized bone fragments (ML)
	30) Osteophytes at patellar ligament insertion on the tibia (ML)
	31) Mineralization of the meniscus (AP)
	32) Intercondylar avulsion fragments (AP)

The radiographic projection for each feature is given in brackets: ML=mediolateral; AP=anteroposterior

Diagnostic imaging studies

Serial radiography and ultrasonography were performed on days 0, 30, 60 and 105.

Conventional radiography of left (OA) and right (control) stifle joints was done in two views: anteroposterior (AP) and mediolateral (ML). The scoring of radiographs was done according to Lazar et al. (2005) recording 32 individual traits (Table 1). The changes were evaluated as absent (0), mild (1), significant (2) and severe (3). The individual scores were thus between 0 and 96 points.

B-mode ultrasonography of stifle joints was performed with diagnostic ultrasounds ALOKA® USG (Japan) with 5.0 MHz linear transducer and CHISON 600 VET (China) with microconvex multifrequency transducer at 7.0 MHz. Joints were examined according to acoustic approaches described by Kramer et al. (1999). Left (OA) and right (control) stifles were scanned in sagittal and transverse plans, both in static position and while moving (extension, flexion, rotation). No sedation was necessary. Sonogrammes were documented on thermovideoprinter Mitsubishi® (Japan). A modification of the scoring system of Muzzi et al. (2009) was used. Individual scores ranged between 0 and 23 points (Table 2).

Individual scores were recorded by two independent observers and the arithmetic mean was retained.

Table 2. Ultrasound scoring system of stifle joints with osteoarthritis (modification of Muzzi et al., 2009).
Tablo 2. Diz ekleminde osteoartiritin ultrason ile skorlama sistemi (Muzzi ve ark., 2009 modifikasyonu ile).

Sign	Score
Joint effusion – presence of anechoic or hypoechoic areas between the tibial Intercondylar area and femoral condyles	0 – absent 1 – mild 2 – moderate 3 – severe 4 - very severe
Intraarticular tissue reaction – presence of fibrous tissue at the insertion point of the cranial cruciate ligament and/or at the cranial intermeniscal ligament	0 – absent 1 – mild 2 – moderate 3 – severe 4 - very severe
Intraarticular inclusion bodies - presence of avulsion osteochondral and/or mineralized joint fragments (bodies with intense homogeneity)	0 - absent 1 - present
Synovial membrane inflammation – thickening (hyperplasia/hypertrophy) in mid-sagittal plane; increased echogenicity	0 - absent 1 - mild 2 - moderate 3 - severe 4 - very severe
Articular cartilage at the condylar bone boundary (mid-sagittal plane)	0 - anechoic 1 - hypoechoic 2 - hyperechoic 3 - heterogeneous
Meniscuses (mid-sagittal plane)	0 - anechoic 1 - hypoechoic 2 - hyperechoic 3 - heterogeneous
Bone surface – irregular and/or rounded interruptions of the hyperechoic boundary of bones	0 - absent 1 - mild 2 - moderate 3 - severe 4 - very severe

Statistical analysis

The results were statistically processed by the non-parametric Friedman and Mann-Whitney tests using Statmost for Windows, Datamost Corp., 1994-1995. Differences less than 0.05 were accepted as statistically significant. **R**elationships between two scores were estimated by the Pearson correlation analysis test.

Results

The serial radiography of knee joints in dogs with experimental chemical model of OA exhibited progressing degenerative changes.

The respective mean scores of OA joints (Table 3) were 13±1.7 by day 30, 28±3.2 by day 60 and 32±4.4 by day 105 ($P<0.01$ vs baseline). The differences between them and contralateral joints scores were considerable ($P<0.01$). The early changes consisted in strong joint effusion and irregularly enlarged intraarticular space. Later changes were related to altered shape and area of bone surfaces, increased density of epiphyseal subchondral zone (sclerosis) and tibial epicondylar focal lysis. Osteophytes were mainly observed on the periphery of joint and the trochlear margin. By the end of the survey period, the subchondral osteosclerosis of both femur and tibia were enhanced and their bone architectonics - entirely changed (Figure 1). The intraarticular space was reduced; the bone margins were irregular and indistinct. At some radiographs, the joint capsule density was increased (fibrosis).

Table 3. Radiological and ultrasound scores in dogs with experimental monoiodoacetate (MIA) model of stifle joint osteoarthritis (mean ± SEM; n=6).

Tablo 3. Deneysel monoiyodoasetat modeli (MIA) ile köpeklerin diz eklemlerinde geliştirilen osteoartiritin radyolojik ve ultrasonografik skorları (ortalama ± SEM; n = 6).

Parameter		Days after the first MIA injection			
		0	30	60	105
Radiological score of stifle joints	Left	0±0.0	13±1.7*	28±3.2*	32±4.4*
	Right	0±0.0	0±0.0#	0±0.0#	1±0.2#
Ultrasound score of stifle joints	Left	1±0.2	19±0.6**	18±1.0**	17±0.8**
	Right	1±0.2	2±0.2#	2±0.2#	2±0.2#

*$P<0.01$ vs baseline (day 0); #$P<0.01$ between left (OA) and right (control) joints.

By ultrasonography, joint effusion occurring by the 30th day in left knees was also visible. Suprapatellar and intercondylar areas were hypo- to anechoic, with homogenous structure. The effusion decreased in later periods. The suprapatellar recess of the joint capsule was hypoechoic, and of larger size as compared to that of the contralateral joint (Figure 2). After the 105th day, fibrosis was already visible appearing with increased echogenicity and heterogeneity, as well as with thickening. The infrapatellar fat body was displaced toward the patellar ligament, moderately echoic and with indistinct borders, without changed size (Figure 2). On this hyperechoic background, the cranial cruciate ligament was delineated as a hypoechoic oblique line. Bone surface was visualized as an irregular hyperechoic line with acoustic shadow behind. Larger osteophytes were seen as distinct discrete hyperechoic structures. The patella was observed as convex hyperreflective object with acoustic window behind, while the patellar ligament was seen in mid-sagittal plane as a hyperechoic fibrillar band. The articular cartilage was an anechoic line near to the bone.

The ultrasound scores of left knee joints were 9±0.6 by day 30, 18±1.0 by day 60 and 17±0.8 by day 105 ($P<0.01$ vs both baseline and vs respective scores of control joints).

Discussion

Radiological signs of OA have been extensively discussed in the literature (Allan, 2007; Bennett, 1990; Carring, 1997; Comerford, 2006). The observed changes vary according to the stage of the disease: effusion, articular space widening followed by narrowing, osteophyte formation, subchondral sclerosis, soft tissue mineralization, subchondral bone cysts, shift of intrapatellar fat body etc. In our experiment, these alterations were observed with a marked tendency towards accumulation and aggravation with progression of the disease.

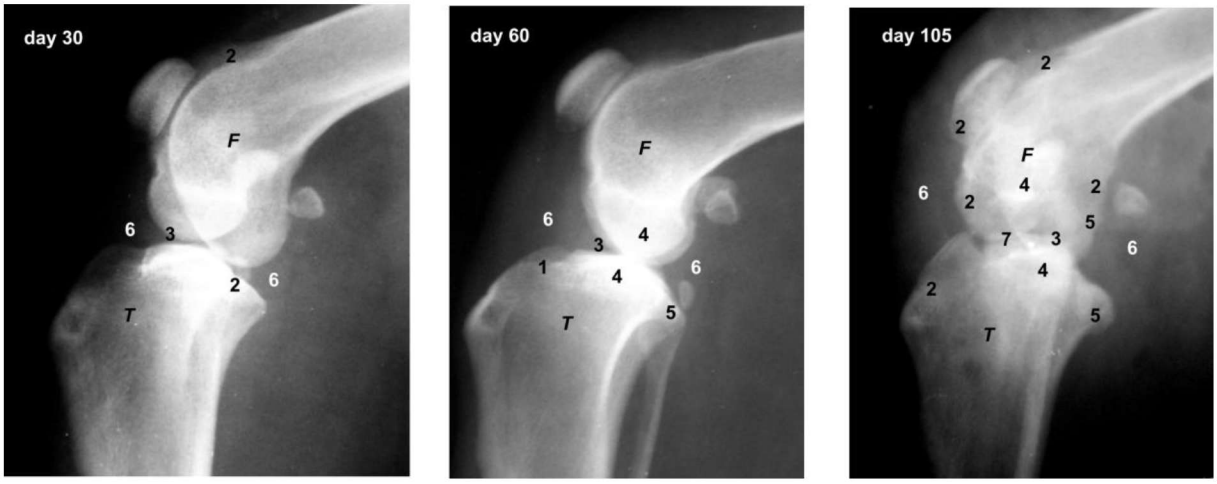

Figure 1. Radiographs of the left stifle joints of dogs with experimental monoiodoacetate model of osteoarthritis 30, 60 and 105 days after the treatment.

Şekil 1. Deneysel monoiyodoasetat modeli (MIA) ile köpeklerin diz eklemlerinde geliştirilen osteoartiritin tedavi sonrası 30., 60. ve 105. günlerde sol eklem radyografileri.

F – femur; T – tibia, 1 –changes in bone positioning; 2 – altered bone margins; 3 – altered intraarticular space; 4 – subchondral osteosclerosis; 5 – osteophytes; 6 – enhanced soft tissue density; 7 – intraarticular inclusion bodies.

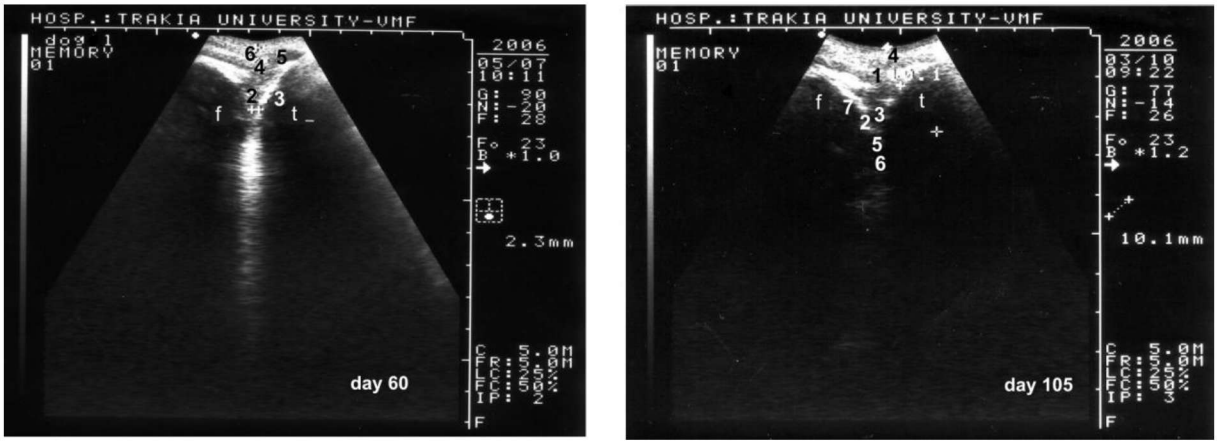

Figure 2. Ultrasonogrammes of the left stifle joints of dogs with experimental monoiodoacetate model of osteoarthritis 60 and 105 days after the treatment.

Şekil 2. Deneysel monoiyodoasetat modeli (MIA) ile köpeklerin diz eklemlerinde geliştirilen osteoartiritin tedavi sonrası 60. ve 105. günlerde sol eklem ultrasonografileri.

F – femur; T – tibia; 1– intraarticular effusion; 2 – intraarticular fibrosis; 3 – intraarticular inclusion bodies; 4 – hypertrophy of jopint capsule and ligaments; 5 – irregular cartilage margins; 6- irregularities of meniscuses; 7- irregularities on bone surfaces.

Although knee joint radiography is an objective method, it is not of primary importance in OA diagnostics. Its role, in the view of Robins (1990), is to detect late symptoms of disease. The fine cartilage defects which are essential for early diagnostics of the condition remain invisible (Widmer et al., 1994).

To the best of our knowledge, this is the first report for successful reproduction of OA in canine knee joint by intraarticular injection of sodium monoiodoacetate and therefore, the observed changes could not be judged against other data reported. The findings were similar to signs described in horses and rats with the same experimental OA model: narrowed intraarticular space, segmentation and disappearing of the tibial contour, trabecular sclerosis, subchondral cysts, osteophytes, extensive bone resorption areas (Morenko et al., 2004; Penraat et al., 2000; Whitton, 2004).

Subchondral cysts are related to advanced OA and often cause lameness in humans and horses (Textor et al., 2001). Their localisation in underlying bone is a source of constant pain and a bad prognostic sign in osteoarthritic horses (Bueno et al., 1999). According to Durr et al. (2004) the cysts were a sequel of cartilage microfractures and subchondral bone stress with secondary resorption. Their formation is rather an exception in our OA model as in general, they are rarely reported in dogs and cats but common in large animals with degenerative joint diseases (Houlton, 1994). Widmer et al. (1994) did not report cystic lesions before the 12th week in dogs with osteoarthritis, but observed them in later stages.

In this study, osteophytes were observed in the second half of the period of survey. According to Widmer et al. (1994) they could not be seen before the 3rd week in dogs as early changes are characterized with synovitis and then, by soft tissue proliferation. The differences between osteoarthritic and healthy joint were radiologically visible between the 6th and the 12th week (Widmer et al. 1994) whereas Innes et al. (2004) reported appearance of osteophytes in the contralateral joint as well after the 13th month.

The dynamic ultrasonography of knee joints, similar to that in men (Kil-Ho Cho, 2001) allowed the detection of the typical degenerative changes in soft tissues in this OA model. Not all findings were seen on a single sonogramme. The sagittal infrapatellar acoustic window in maximally flexed joint was the most appropriate. Using a convex 7.0 MHz transducer, we obtained the best results as reported by Gnudi et al. (2001), Kramer et al. (1999), Reed et al. (1995) and Muzzi et al. (2009) for knee joint structures in dogs. This experimental OA model was characterized with inflammatory onset – intraarticular effusion and swelling of the suprapatellar joint recess, and later, by degeneration (bone contour segmentation). In the middle of the survey period, fibrosis, cartilage fragmentation, menisci protrusion and bone affections were predominant. The thickening of the synovial layer of the joint capsule was a constant echography finding. By means of 5-7.5 MHz transducers, Kramer and Gerwing (1996) have detected effusion, thickening, fibrosis and osteochondral lesions in canine shoulder and stifle joints, as well as joint instability by means of dynamic scanning.

The correlation analysis showed a statistically significant positive relationship between signs which are specific for one imaging technique (radiography or ultrasonography) and could not be detected by the other. Therefore, the detected symptoms of disease are more numerous and the picture of osteoarthritis – more detailed, if both diagnostic imaging methods are combined.

Conclusion

Diagnostic imaging studies in the used chemical (monoiodoacetate) experimental model of osteoarthritis revealed dynamic progressive changes in treated knee joints, typical for the naturally occurring disease.

Radiography visualized mainly late bone changes (osteophytes, subchondral bone sclerosis, cysts, remodelling) by the 2nd-3rd

month. The ultrasonography was useful in detecting early changes in soft articular tissues (effusion, cartilage defects, and capsule fibrosis). The strong correlation between radiological and ultrasound knee joint scores suggested that the combined use of both diagnostic imaging techniques was more beneficial to obtain a detailed insight into canine osteoarthritis.

REFERENCES

Abercromby, R., Innes, J., May, C., 2006. Arthritis. In: Houlton J., Cook J., Innes J., Langley-Hobbs S., Brown G. (Eds). BSAVA Manual of Canine and Feline Musculoskeletal Disorders, Glochester, England, pp. 81-109.

Allan, G., 2007. Radiographic signs of joint disease in dogs and cats. In: Donald Thrall (Ed.), Textbook of Veterinary Diagnostic Radiology, 5th Edition, Saunders Elsevier Philadilphia, PA, USA, chapter 18, pp. 317-358.

Bennett, D., 1990. Diagnosis of joint disease. Joints and joint diseases. In: Whittick W. (Ed). Canine Orthopedics, 2nd Edition, Section 4, 1990, chapter 24, pp. 761-833.

Bennett, D., Tennant, B., Lewis, D., Baughan, J., May, C., Carter, S., 1988. A reappraisal of anterior cruciate ligament disease in the dog. Journal of Small Animal Practice 29, 275-297.

Boulos, P., Papaioannou, A., Beattie, K., Adachi, J., 2003. Measurement techniques for the detection of early osteoarthritis. Business briefing: North American Pharmacotherapy, reference section. 1-5.

Buckwalter, J., Martin, J., 2006. Osteoarthritis. Journal of Advanced Drug Delivery Reviews 58 (2), 150-167.

Budsberg, S., Thomas, M., 2006. Advanced diagnostic techniques. In: Houlton J., Cook J., Innes, J., Langley-Hobbs, S., Brown, G. (Eds). BSAVA Manual of Canine and Feline Musculoskeletal Disorders, Glochester, England, pp. 27-33.

Bueno, A., Kaneps, A., Watrous, B., 1999. Vet Med Today: What is Your Diagnosis? Journal of the American Veterinary Medical Association 215 (8), 1097-1098.

Carring, C., 1997. Diagnostic inaging of osteoarthritis. Veterinary Clinics of North America 27 (4), 777-814.

Comerford, E., 2006. The Stifle Joint. In: Barr F. and Kirberger R. (Eds). BSAVA Manual of Canine and Feline Musculosceletal Imaging, Glouchester, England, pp. 135-149.

Durr, H., Martin, H., Pellengahr, C., Schlemmer, M., Maier, M., Jansson, V., 2004. The cause of subchondral bone cyst in osteoarthrosis. A finite element analysis. Acta Orthopaedica Scandinavica 75 (5), 554-558.

Ehrlich, G., 2003. The rise of osteoarthritis. Bulletion of the World Health Organization 81 (9), 630.

Gnudi, G., Bertoni, G., 2001. Echographic examination of the stifle joint affected by cranial cruciate ligament rupture in the dog. Veterinary Radiology and Ultrasound 42 (3), 266-270.

Grainger, R., Cicuttini, F., 2004. Medical management of osteoarthritis of the knee and hip joints. The Medical Journal of Australia 180 (3), 232-236.

Grassi, W., Cervini, C., 1998. Ultrasonography in rheumatology: An evolving technique. Annals of the Rheumatic Diseases 57, 268-271.

Haima, P., 2005. Biochemical markers for the management of rheumatoid arthritis and osteoarthritis. Osteomedical group. Clinical and Technical Monograph 1-28.

Houlton, J., 1994. Ancillary aids to the diagnosis of joint disease. Analysis of synovial fluid. In: Houlton J. and Collinson R. (Eds). Manual of Small Animal Arthrology BSAVA, pp. 22-38.

Innes, J., Costello, M., Barr, F., Rudorf, H., Barr, A., 2004. Radiographic progression of osteoarthritis of the canine stifle joint: A prospective study. Veterinary Radiology and Ultrasound 45 (2), 143-148.

Kil-Ho Cho, Dong-Chul Lee, Rethy Kieth Chhem, Jose Antonio Bouffard, Etienne Cardinal, Bok-Hwan Park, 2001. Normal and acutely torn posterior cruciate ligament of the knee at US evaluation: Preliminary experience. Radiology 219, 375-380.

Kramer, M., Gerwing, M., 1996. The importance of the sonography in the orthopedic problems in dogs. Berliner und Münchener Tierärztliche Wochenschrift 109, 130-135.

Kramer, M., Gerwing, M., Hach, V., Shumke, E., 1997. Sonography of the musculoskeletal system in dogs and cats. Veterinary Radiology and Ultrasound 38 (2), 139-149.

Kramer, M., Stengel, H., Gerwing, M., Schumke, E., Sheppard, C., 1999. Sonography of the canine stifle. Veterinary Radiology and Ultrasound 40 (3), 282-293.

Lazar, T., Berry, C., Dehaan, J., Peck, J., Correa, M., 2005. Long-term radiographic comparison of tibial plateau leveling osteotomy versus extracapsular stabilization for cranial cruciate ligament rupture in the dog. Veterinary Surgery 34, 133-141.

Lipowitz, A., 1993. Degenerative joint disease. Musculoskeletal system, sec.15. In: Douglas Slatter (Ed).. Textbook of Small Animal Surgery, vol. II; 2nd Edition, Philadelphia, USA, pp. 1921-1927.

Martel-Pelletier, J., Reginster, J., 1999. The influence of tissular cross-talking on osteoarthritis progression: role of nonsteroidal antiinflamatory drugs. Osteoarthrtis and Cartilage 7, 306-307.

May, S., 1994. Degenerative joint disease (osteoarthritis, osteoarthrosis, secondary joint disease). In: Houlton J. and Collinson R. (Eds). Manual of Small Animal Arthrology, BSAVA, chapter 5, pp. 62-73.

Morenko, B., Bove, S., Chen, L., Guzman, R., Juneau, P., Bocan, T., Peter, G., Arora, A., Kilgore, K., 2004. In vivo micro computed tomography of subchondral bone in the rat after intra-articular administration of monosodium iodoacetate. Contemporary Topics in Laboratory Animal Science, 43 (1), 39-43.

Muller, S., Kramer, M., 2003. The use of ultrasonography in the diagnostic of meniscus lesions in the dog. Tierarztlische Praxis, 31, 10-15.

Muzzi, L., Rezende, C., Muzzi, R., 2009. Physiotherapy after arthroscopic repair of the cranial cruciate ligament in dogs. I – clinical, radiographic, and ultrasonographic evaluation. Arquivo Brasileiro de Medicina Veterinária e Zootecnia 61 (4), 805-814.

Penraat, J., Allen, A., Fretz, P., Bailey, J., 2000. An evaluation of chemical arthrodesis of the proximal interphalangeal joint in the horse by using monoiodoacetate. The Canadian Journal of Veterinary Research 64, 212-221.

Railhac, J., Vial, J., 2007. Cartilage imaging: The example of osteoarthritis of the knee. In: Assessing osteoarthritis. Bulletin International du Mouvement, 6, 7-11. www.observatoire-du-mouvement.com.

Reed, A., Payne, J., Constantinescu, G., 1995. Ultrasonographic anatomy of the normal canine stifle. Veterinary Radiology and Ultrasound, 36 (4), 315-321.

Robins, G., 1990. The canine stifle joint. In: Wiliam G. Whittick (Ed). Canine Orthopedics, section VI: Joint disorders, ch. 23, 693-760.

Swagerty, D., Hellinger, D., 2001. Radiographic Assessment of Osteoarthritis. The American Family Physician 64, 279-286.

Textor, J., Nixon, A., Lumsden, J., Ducharme, N., 2001. Subchondral cystic lesions of the proximal extermity of the tibia in horses: 12 cases (1983-2000). Journal of the American Veterinary Medical Association 218 (3), 408-413.

Torelli, S., Rahal, S., Volpi, R., Sequera, J., Grassioto, I., 2005. Histopathological evaluation of treatment with chondroitin sulphate for osteoarthritis induced by continious immobilization in rabbits. Journal of Veterinary Medicine series A 52 (1), 45-51.

Van Bree, H., 2006. Diagnistic imaging of orthopaedic problems in small animals: A practical guide. IAMS Clinical Nutrition Symposium, 7-13, www.vetcontact.com/iams_symposium2006/vanbree.pdf.

Vasseur, P., 1993. Stifle joint. In: D. Slatter (Ed). Textbook of Small Animal Surgery, 2nd Edition, vol.II, ch.137, pp. 1817-1862.

Whitton, C., 2004. Chemical arthrodesis of the distal tarsal joints using sodium monoiodoacetate in 104 horses. The Australian Veterinary Journal 82 (5), 286-287.

Widmer, R., Buckwalter, K., Braunstain, E., Hill, M., O`Connor, M., Visco, D., 1994. Radiographic and magnetic resonance imaging of the stifle joint in experimental osteoarthritis of dogs. Veterinary Radiology and Ultrasound 35 (5), 371-383.